SC5361.8SA

AFOSR-TR-[illegible]

SC5361.8SA

Copy No. 5

(2)

NONLINEAR WAVE PROPAGATION STUDY

SEMI-ANNUAL TECHNICAL REPORT NO. 3 FOR THE PERIOD December 1, 1984 through May 31, 1985

CONTRACT NO. F49620-83-C-0065
DARPA ORDER NO. 4400
PROGRAM CODE: 3A10

Prepared for

Air Force Office of Scientific Research
Building 410
Bolling AFB, DC 20332

Prepared by

J.R. Bulau
805-373-4153
and
B.R. Tittmann

Sponsored by

Defense Advanced Research Projects Agency (DoD)
DARPA Order No. 4400
Monitored by NP Under Contract No. F49620-83-C-0065

Rockwell International
Science Center

UNCLASSIFIED
SECURITY CLASSIFICATION OF THIS PAGE

REPORT DOCUMENTATION PAGE

1a. REPORT SECURITY CLASSIFICATION Unclassified	1b. RESTRICTIVE MARKINGS
2a. SECURITY CLASSIFICATION AUTHORITY	3. DISTRIBUTION/AVAILABILITY OF REPORT Approved for public release; distribution unlimited.
2b. DECLASSIFICATION/DOWNGRADING SCHEDULE	
4. PERFORMING ORGANIZATION REPORT NUMBER(S) SC5361.8SA	5. MONITORING ORGANIZATION REPORT NUMBER(S)
6a. NAME OF PERFORMING ORGANIZATION Rockwell International Science Center 6b. OFFICE SYMBOL (If applicable)	7a. NAME OF MONITORING ORGANIZATION same as #8
6c. ADDRESS (City, State and ZIP Code) 1049 Camino Dos Rios Thousand Oaks, CA 91360	7b. ADDRESS (City, State and ZIP Code)
8a. NAME OF FUNDING/SPONSORING ORGANIZATION Air Force Office of Scientific Research 8b. OFFICE SYMBOL (If applicable)	9. PROCUREMENT INSTRUMENT IDENTIFICATION NUMBER Contract No. F49620-83-C-0065
8c. ADDRESS (City, State and ZIP Code) Building 410 Bolling AFB, DC 20332	10. SOURCE OF FUNDING NOS PROGRAM ELEMENT NO. DARPA ORDER NO. 4400 / PROJECT NO. 3A10 / TASK NO. / WORK UNIT NO.
11. TITLE (Include Security Classification) NON-LINEAR WAVE PROPAGATION STUDY (U)	
12. PERSONAL AUTHOR(S) Bulau, J.R. and Tittmann, B.R.	
13a. TYPE OF REPORT Semi-Annual Technical No. 3	13b. TIME COVERED FROM 12/01/84 TO 05/31/85
14. DATE OF REPORT (Yr., Mo., Day) JULY 1985	15. PAGE COUNT 38

16. SUPPLEMENTARY NOTATION
The views and conclusions contained in this document are those of the authors and should not be interpreted as necessarily representing the official policies, either expressed or implied, of the Defense Advanced Research Projects Agency or the U.S. Government.

17. COSATI CODES		
FIELD	GROUP	SUB. GR.

18. SUBJECT TERMS (Continue on reverse if necessary and identify by block number)

19. ABSTRACT (Continue on reverse if necessary and identify by block number)
In this document we report the results of combined high amplitude tensile and compressive loading experiments on four different rock types: Westerly granite, Boise sandstone, Berea sandstone, and Indiana limestone. The details of the stress-strain hysteresis loops are examined, with emphasis on investigating the elastic and inelastic properties of rocks at nonlinear amplitudes in both tension and compression. The results indicate that the mechanical behavior of rocks can be significantly different in compression than in tension and that the onset of nonlinear effects with increasing strain may not be the same for compressive loads as for tensile loads. All available evidence indicates that the primary relaxation mechanism at nonlinear amplitudes between 10^{-6} strain and 10^{-4} strain involves intergranular friction. More experimental work in this area will shed light on the issue of linearity vs. nonlinearity at intermediate strains, and also will provide realistic detailed information about rock rheology for the numerical modeling of near-field seismic pulse propagation.

20. DISTRIBUTION/AVAILABILITY OF ABSTRACT UNCLASSIFIED/UNLIMITED ☒ SAME AS RPT. ☐ DTIC USERS ☐	21. ABSTRACT SECURITY CLASSIFICATION Unclassified
22a. NAME OF RESPONSIBLE INDIVIDUAL William Best	22b. TELEPHONE NUMBER (Include Area Code) (202) 767-4908 / 22c. OFFICE SYMBOL NP

DD FORM 1473, 83 APR EDITION OF 1 JAN 73 IS OBSOLETE.

UNCLASSIFIED
SECURITY CLASSIFICATION OF THIS PAGE

TABLE OF CONTENTS

		Page
1.0	SUMMARY	1
2.0	INTRODUCTION	3
3.0	EXPERIMENTAL PROCEDURES	8
4.0	EXPERIMENTAL RESULTS	11
5.0	DISCUSSION AND CONCLUSIONS	30
6.0	REFERENCES	31

LIST OF FIGURES

Figure		Page
3.1	Schematic illustration of the apparatus used for the measurement of stress-strain response curves. (a) MTS electro-hydraulic load frame and (b) detail of sample and end fixtures....	8
3.2	Schematic illustration of instrumentation used to acquire and process stress-strain response curves.....	9
3.3	Representative stress loading functions with corresponding strain response functions for (a) aluminum bar with a peak stress of $\pm$ 1.32 $\times 10^7$ Pa and (b) Boise sandstone with a peak stress of 4.38 $\times 10^7$ Pa.....	10
4.1	Stress-strain response for aluminum test bar.....	11
4.2	Stress-strain response for Boise sandstone with a peak loading stress of 4.5 $\times 10^4$ Pa showing nearly linear behavior.....	13
4.3	Stress-strain response for Berea sandstone with a peak loading stress of 4.5 $\times 10^4$ Pa showing nearly linear behavior.....	13
4.4	Stress-strain response for Westerly granite with a peak loading stress of 4.5 $\times 10^4$ Pa showing nearly linear behavior.....	14
4.5	Stress-strain response for Indiana limestone with a peak loading stress of 4.5 $\times 10^4$ Pa showing nearly linear behavior.....	14
4.6	Stress-strain response for Boise sandstone with a peak loading stress of 1.32 $\times 10^6$ Pa.....	15
4.7	Stress-strain response for Berea sandstone with a peak loading stress of 1.32 $\times 10^6$ Pa.....	15
4.8	Stress-strain response for Westerly granite with a peak loading stress of 1.32 $\times 10^6$ Pa.....	16
4.9	Stress-strain response for Indiana limestone with a peak loading stress of 1.32 $\times 10^6$ Pa.....	16
4.10	Stress-strain response for two rocks showing the anomalous occurrence of a slightly higher effective modulus in tension than in compression. Peak loading stresses are relatively small (1.32 $\times 10^5$ Pa) in each case.....	17
4.11	Magnified views of the hysteresis loop tips for Westerly granite.	18

LIST OF FIGURES (Continued)

Figure		Page
4.12	Magnified views of the hysteresis loop tips for Boise sandstone...	19
4.13	Magnified views of the hysteresis loop tips for Berea sandstone...	20
4.14	Comparison of the first loading cycle for Berea sandstone at 1.25×10^6 Pa with the subsequent 7 cycles showing nonrecoverable changes after the first. The previous maximum load was 4.39×10^5 Pa.....	21
4.15	Stress-strain response for the first eight loading cycles for Boise sandstone at 1.25×10^6 Pa. A small amount of nonrecoverable change is observed after the first cycle, but the following seven are superimposed. The previous maximum load was 4.39×10^5 Pa...	22
4.16	Stress-strain response for the first eight loading cycles for Westerly granite at 1.25×10^6 Pa. A small amount of nonrecoverable change is observed after the first cycle, but the following seven are superimposed. The previous maximum load was 4.39×10^5 Pa....	22
4.17	Stress-strain response for the first eight loading cycles for Indiana limestone at 1.25×10^6 Pa. The material appears to be nearly linear elastic and nonrecoverable changes are not observed.	23
4.18	Effect of reversing the initial loading direction from tension-first to compression-first for Boise sandstone with a maximum loading stress of 4.39×10^6 Pa, showing the lack of significant hysteresis in the compressional part of the cycle.....	24
4.19	Effect of reversing the initial loading direction from compression-first to tension-first for Boise sandstone with a maximum loading stress of 4.39×10^6 Pa, showing the development of a hysteresis loop in tension.....	25
4.20	Effect of reversing the initial loading direction from tension-first to compression-first for Westerly granite with a maximum loading stress of 4.39×10^6 Pa, showing a significant compressional hysteresis loop.....	26
4.21	Effect of reversing the initial loading direction from compression-first to tension-first for Westerly granite with a maximum loading stress of 4.39×10^6 Pa. Figure shows the existence of a hysteresis loop in tension which is larger than the compressional hysteresis loop illustrated in Fig. 4.20.....	27

LIST OF FIGURES (Continued)

Figure — Page

4.22 Comparison of the stress-strain response for Berea sandstone at two different frequencies. The traces appear to be identical..... 28

4.23 Comparison of the stress-strain response for Westerly granite at two different frequencies. The traces appear to be identical..... 29

1.0 SUMMARY

In an effort to better understand the mechanics of wave propagation through the near field of an explosive seismic source, the real time functions of stress and strain have been measured for a variety of rock types using both tensile and compressive loading. Experiments were performed using cylindrical specimens of Boise sandstone, Berea sandstone, Indiana limestone, and Westerly granite. Peak stresses varied from 4.5×10^4 Pa to 2.5×10^6 Pa, and maximum longitudinal strains, as measured on the surface of the cylinders, varied from approximately 1×10^{-6} to 2×10^{-4}. Differences in the details of the experimental results exist among the various rock types studied, but the following observations are generally applicable:

1. At very low amplitudes the rocks behave almost linearly; the stress-strain curves have the same slope on either side of zero stress, and a hysteresis loop cannot be detected above the noise level.

2. The first evidence of nonlinearity appears at peak stresses of approximately 1×10^5 Pa. At this amplitude the slope of the stress-strain relationship is not the same on either side of zero stress. In all but two anomalous cases, Indiana limestone and Westerly granite at relatively low peak stress levels, the effective modulus is higher in compression than in tension. Furthermore, a small hysteresis loop is observed, especially on the tensile side of zero stress.

3. Hysteresis loops continue to enlarge with increasing maximum stress. Compressional hysteresis loops are smaller than tensional loops, and nonlinearity is obvious.

These results confirm that nonlinear effects are present in rocks at very low amplitudes ($<10^5$ Pa stress and $<10^{-5}$ strain) both in compression and in tension. Material response in compression is more elastic than in tension, in that the loading-release curve follows a curved path, but with relatively little hysteresis. A significant amount of hysteresis is observed in tension. This is apparently related to intergranular friction, which is aided by the opening of intergranular cracks. Measurements using the resonating bar technique, as reported previously, are excellent for detecting the first signs of nonlinearity in either tension or extension, but cannot resolve differences in extensional behavior vs compressional behavior. Finally, it is unlikely that rocks respond perfectly linearly to high amplitude compressive pulses propagating through the near field of an explosion at peak stresses greater than approximately 10^5 Pa. It is more likely that material response is nonlinear in compression, with a small amount of hysteresis due to intergranular friction. Further studies of rocks are planned while the specimens are subjected to elevated effective stresses in order to test this hypothesis.

2.0 INTRODUCTION

The mechanics of wave propagation through the near field of an explosive seismic source are not completely understood, particularly in the peak strain amplitude range between 10^{-4} and 10^{-6}. The most complete data sets which describe free-field wave propagation as a function of scaled distance (distance/yield$^{1/3}$) in this strain amplitude range have been obtained for explosions in polycrystalline salt. The data base includes measurements from (a) the 5.3 kT nuclear event, SALMON (Perret, 1967; Trulio, 1978); (b) the medium to large scale chemical explosions of the COWBOY experiments, which took place in a natural salt dome (Trulio, 1978, 1981); and (c) a series of small scale chemical explosions in pressed polycrystalline salt in the laboratory (Larson, 1982). When all available data are combined, wave propagation appears to satisfy cube root of yield scaling. That is, the decay of peak particle velocity and displacement can be defined as a function of distance/yield$^{1/3}$ (Trulio, 1978, 1981; Larson, 1982). This appears to be the case, even though available data cover approximately 10 decades in yield, 4 decades in peak particle velocity, and 4 decades in frequency. However, the data fit a line that decays much faster than r^{-1}, which would be the case if the material behaves in a perfectly elastic manner. Thus, the behavior of salt in the range of available free field measurements, to strains as low as approximately 7×10^{-6}, cannot be regarded as perfectly elastic (Trulio, 1978. 1981). Because of the uncertainties regarding the amount of energy that can be dissipated as a seismic pulse propagates at intermediate strains, Bache, et al, (1981) have questioned the usefulness of reduced displacement potential (RDP) calculations based on close range data for the purpose of defining a seismic source function.

The exact nature of attenuation in the near field of an explosive seismic source remains a controversial subject. In fact, the evidence regarding the issue of linearity is ambiguous. Using small-scale chemical explosions in pressed salt in the laboratory, Larson (1982) measured a Q of 12.5 near 10^{-3} strain, and a Q of 24.9 near 6×10^{-4} strain. The fact that Q

is amplitude dependent is evidence for nonlinear response. However, Larson also demonstrated an approximately linear superposition of waveforms at strains higher than 10^{-4}, which suggests near-linearity. The experimental results reported in Tittmann (1983) using resonating bars of natural halite indicate that the linear anelastic Q of halite is quite high, near 500, with a transition to an amplitude dependent nonlinear Q at strain amplitudes greater than approximately 2×10^{-6}. Burdick, et al (1984a) have argued that it is possible to model a seismic source function for the Amchitka tests, detonated in volcanic material, assuming linear behavior in the near field just outside the spall zone (approx. 700-1200 $m/kT^{1/3}$). Furthermore, Burdick, et al, (1984b) contend that the same model can be used to predict the first vertical pulse arrival and rise times even within the spall zone. They used the concept of a compressional elastic radius that in fact may be considerably smaller than a tensional elastic radius and that must extend at least as far as the outer limits of the spall zone. Minster and Day (1985) recently re-examined the COWBOY data set, and concluded that it is possible to explain simultaneously the radial decay of peak displacement and peak velocity by either (a) a linear anelastic model with low Q (approx. 20) or (b) a nonlinear model with amplitude dependent Q. MacCarter and Wortman (1985) conclude that the free field motion measurements from the SALMON event are consistent with an amplitude independent Q of about 10. In any case, these amplitude independent Q values are too low to represent the linear anelastic Q of salt according to the results of Tittmann (1983).

While generally it is acknowledged that Q is defined rigorously only when the material through which a wave propagates behaves linearly, it is common (McCarter and Wortman, 1985; Minster and Day, 1985) to assume for theoretical purposes that "nonlinear Q" can be defined using the equations of Mavko (1979) and Stewart, et al (1983):

$$Q^{-1}(\omega, \varepsilon) = Q_0^{-1}(\omega) + \alpha\varepsilon \qquad (1)$$

where Q^{-1} is nonlinear Q, Q_0^{-1} is linear anelastic Q, α is a constant, and ε is strain. This equation considers the combined effects of Coulomb-type friction from many intergranular contacts on the energy dissipated during one full elastic wave cycle. In their derivations, Q^{-1} was defined as

$$Q^{-1} = (1/2\pi)(\Delta W/W) \qquad (2)$$

where ΔW is the energy dissipated in one full cycle, and W is the peak strain energy stored per cycle.

One technique used in the laboratory to estimate nonlinear Q involves the forced resonance of bars. As pointed out in previous reports (Tittmann, 1983a, 1983b, 1984), the various resonating bar techniques offer a particularly sensitive tool for detecting the onset of nonlinearity, even at very low strains. The data reported by Tittmann (1983a) indicate that the intrinsic linear attenuation of dome salt is quite low ($Q > 500$), and that the onset for nonlinear behavior is near 2×10^{-6} strain, corresponding to approximately 1 bar of stress. Similar behavior has been reported for other rock types, including granite, limestones, sandstones, and miscellaneous igneous rocks (cf Mavko, 1979; Stewart et al, 1983). These measurements suggest that nonlinear response should persist to large scaled distances from explosions, on the order of 104 $m/kt^{1/3}$. Furthermore, the low Q values calculated by Larson (1982) [laboratory measurements], Trulio (1979, 1981) [COWBOY], Minster and Day (1985) [COWBOY] and McCarter and Wortman (1985) [COWBOY, SALMON] from free field measurements in salt are much lower. This constitutes additional evidence of nonlinearity in available free-field measurements.

It is also quite tempting to use the nonlinear Q measurements reported from forced resonance-type experiments to estimate the coefficient in Eq. (1). There are certain dangers in doing this, however. First, it must be recognized that resonating bar specimens are not subjected to homogeneous strain. This is not a problem as long as material response is linear. However, it tends to lead to an underestimation of the value of α. Minster and

Day (1985) indicate α that from flexural resonance measurements is probably underestimated by about a factor of 2, and from torsional measurements it is underestimated by about a factor of 3. A second hazard with using nonlinear Q values from resonance measurements is related to the fact that Q is calculated from the bandwidth of the resonance peak, assuming linear anelastic behavior. The distortion of the resonance peak shape associated with nonlinear resonances has been described by Tittmann (1983b) and casts an element of suspicion on the significance of the nonlinear Q values reported. Finally, during both extensional and flexural resonances each increment of volume within the specimen is subjected to tensile stresses half of the time and to compressive stresses the other half. A tacit assumption is that the material behaves the same in compression as it does in tension. The apparent drop in bar modulus with increasing vibration amplitude has been noted (Tittmann, 1983a, 1983b, 1984), and is probably also related to the distortion of the resonance peak shape with increasing strain. Not proven, however, is whether either the frictional losses or the effective modulus of a rock are the same in tension as they are in compression. Resonating bar-type measurements are not capable of resolving the details of the rheological response of materials to nonlinear loading.

On the basis of the above discussion, the laboratory work most beneficial to resolving the issue of linearity vs nonlinearity would involve studies of the mechanical response of various test site materials, including salt, to realistic seismic pulse loading histories. Such studies would necessarily require the application of true uniaxial strain while test specimens are subjected simutaneously to a hydrostatic bias stress. This type of study is very difficult technically, and results of such studies do not exist, at least not in the open literature. Several papers have examined the details of stress-strain hysteresis loops under nonlinear, uniaxial stress loading conditions (distinguished from uniaxial strain) (Gordon and Davis, 1968; McKavanagh and Stacey, 1974), but in each of these cases only compressional measurements were performed. Shock and Louis (1982) examined the inelastic response of two rock types, sandstone and granite, to high tensile stress loading, but did not

examine hysteresis, per se. Nor was the behavior in axial compression contrasted with the behavior in tension.

In this report we describe the results of combined high amplitude tensile and compressive uniaxial stress loading experiments on four different rock types: Westerly granite, Boise sandstone, Berea sandstone, and Indiana limestone, under ambient pressure conditions. This represents the first stage of a new effort with the ultimate goal to examine the mechanical response of test site materials, including dome salt, to high amplitude uniaxial strain loading at elevated hydrostatic pressures. We examine the details of the stress-strain hysteresis loops, and demonstrate that both the elastic and the inelastic properties of rocks at nonlinear amplitudes are quite different in compression than in tension. Results to date indicate that the behavior in compression at strains greater than 10^{-5} is nonlinear, but with much less hysteresis than in tension. The behavior in tension at comparable strains is also nonlinear, but a relatively large hysteresis loop is evident. This indicates that frictional losses are much greater in tensile loading than in compressive loading.

3.0 EXPERIMENTAL PROCEDURES

Figure 3.1 includes schematic illustrations of the mechanical parts of the system used for measurement. Briefly, cylindrical rock specimens 2.54 *cm* in dia. and 6.35 *cm* long were cut from blocks of Boise sandstone, Berea sandstone, Westerly granite, and Indiana limestone. A resistance-type strain gauge was bonded to the surface of each specimen to respond to strains in the longitudinal direction. The rock was then bonded adhesively to stainless steel mounting fixtures using a semiplastic polymer resin (Crystal Bond #509, Aremco Products) that is quite brittle and stiff at room temperature, but that softens readily at approximately 70°C. By keeping the specimen warm while mounting it in the apparatus, residual stresses could be removed. Measurements were made at room temperature and under ambient pressure conditions.

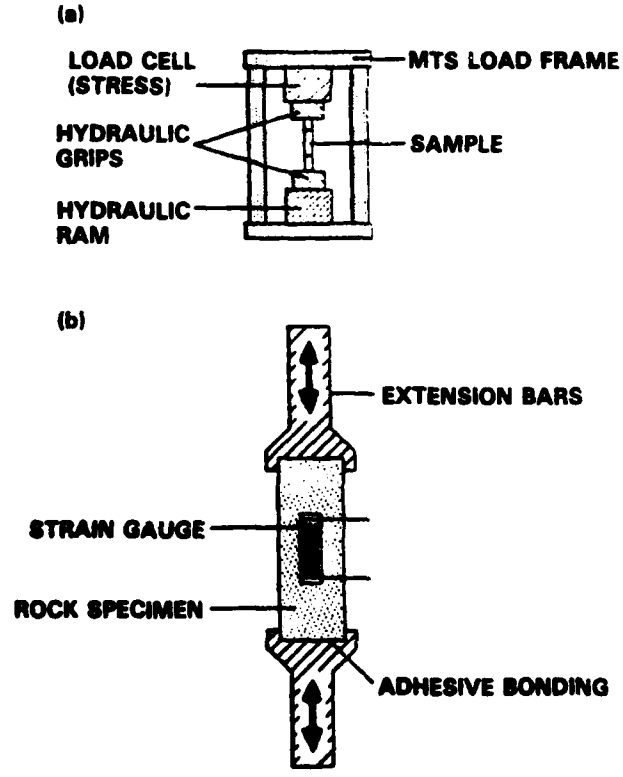

Fig. 3.1 Schematic illustration of the apparatus used for the measurement of stress-strain response curves.

Experiments were run using an MTS electro-hydraulic, closed-loop load frame equipped with the hydraulic hardware and controls necessary to apply alternating tensile and compressive loads. The instrumentation used for the measurements is illustrated in Fig. 3.2. The frequency of loading was usually 1 Hz, except for two series of measurements on Westerly granite and Berea sandstone at 0.1 Hz. A series of eight cycle bursts of load-controlled constant strain rate triangle wave loading were applied to each specimen. Measurements of load and strain were collected simultaneously, digitized, and stored in the computer.

Representative time functions of stress and strain are illustrated in Fig. 3.3. Measurements were obtained on each sample using bursts of increasing maximum stress, starting with $\pm$ 3.4 $\times 10^5$ Pa and working up to a maximum of $\pm$ 3.4 $\times 10^7$ Pa, unless precluded by the breakage of the specimen. As many as 5 bursts of 8 waves each were applied at low amplitudes in order to enable satisfactory signal averaging when the signal-to-noise ratio was low. At higher amplitudes the signal-to-noise ratio was good, and only one eight-cycle burst was run in order to avoid excessive damage to the specimen.

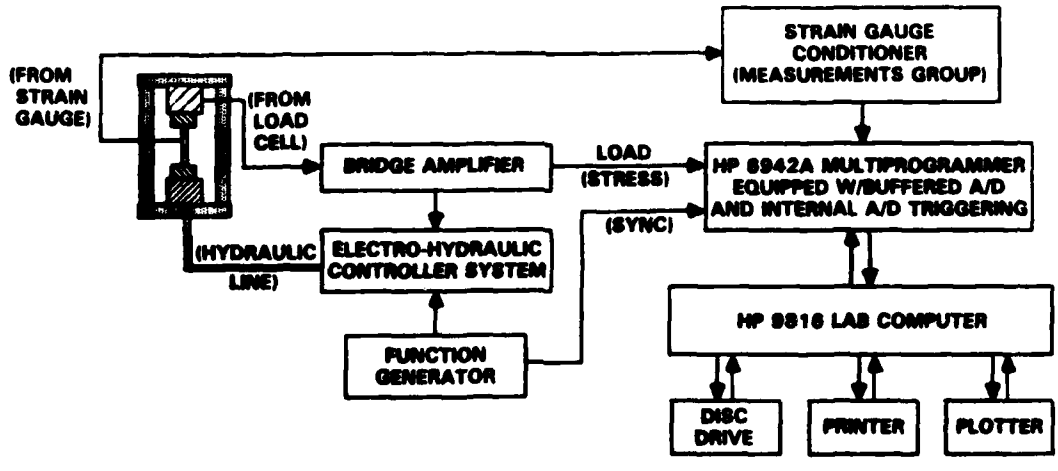

Fig. 3.2 Schematic illustration of instrumentation used to acquire and process stress-strain response curves.

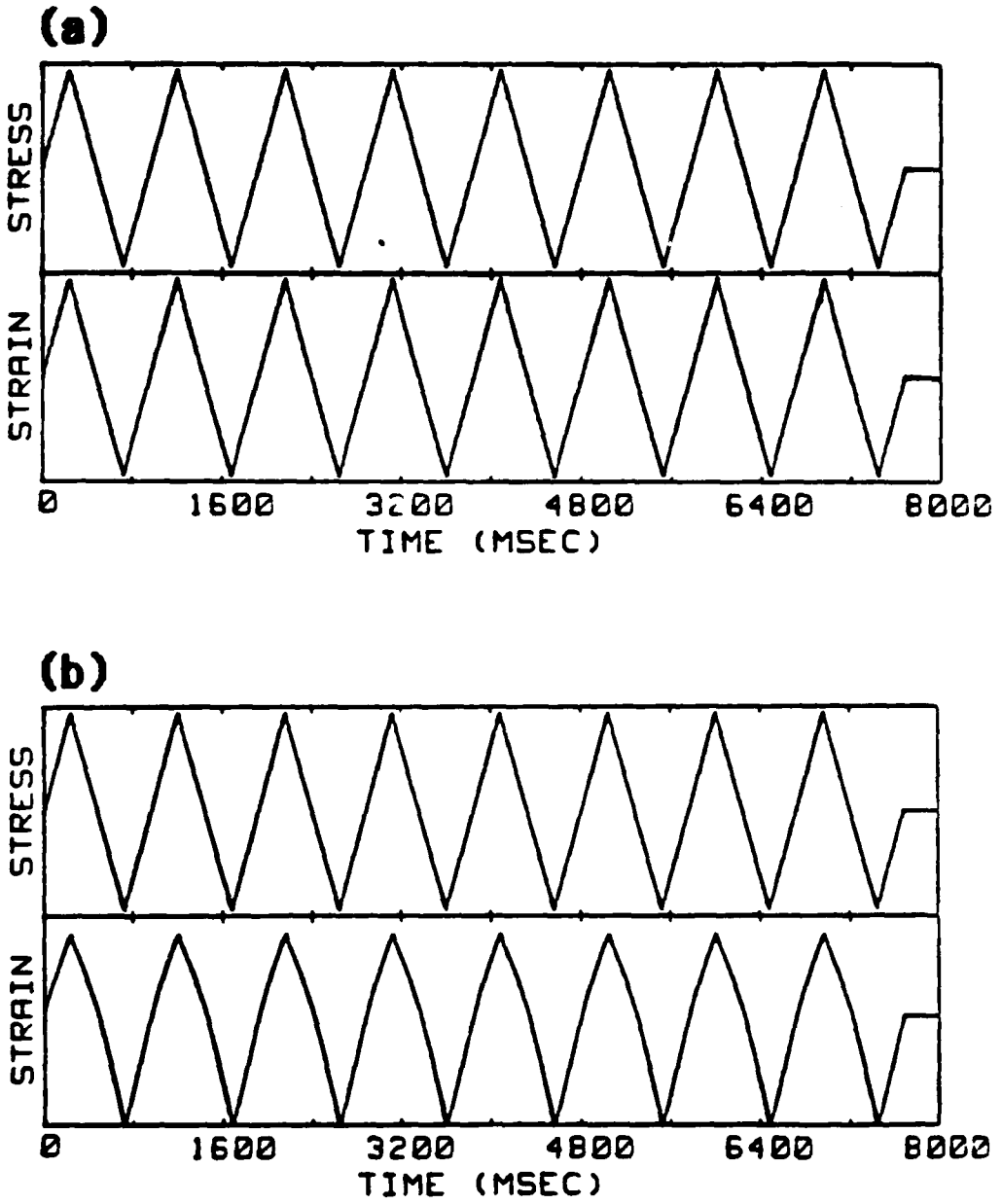

Fig. 3.3 Representative stress loading functions with corresponding strain response curves. (a) MTS electro-hydraulic load fram and (b) detail of sample and end fixtures.

4.0 EXPERIMENTAL RESULTS

To test the linearity of the experimental apparatus and the stiffness of the adhesive bonds, the first phase of the experimental study involved measurements of stress and strain on an aluminum bar which has a relatively ideal linear elastic response. A typical curve of stress vs. strain for an aluminum bar is shown in Fig. 4.1. Extensional stresses and strains are positive. Only a small amount of hysteresis is observed in this set of measurements, and the apparent relationship between stress and strain is nearly linear. A small amount of hysteresis is observed and may be attributed to plastic flow in the resin used to bond the aluminum bar to the loading fixtures. This is a relatively insignificant effect compared with the large amounts of hysteresis and nonlinearity observed in rocks under corresponding stresses.

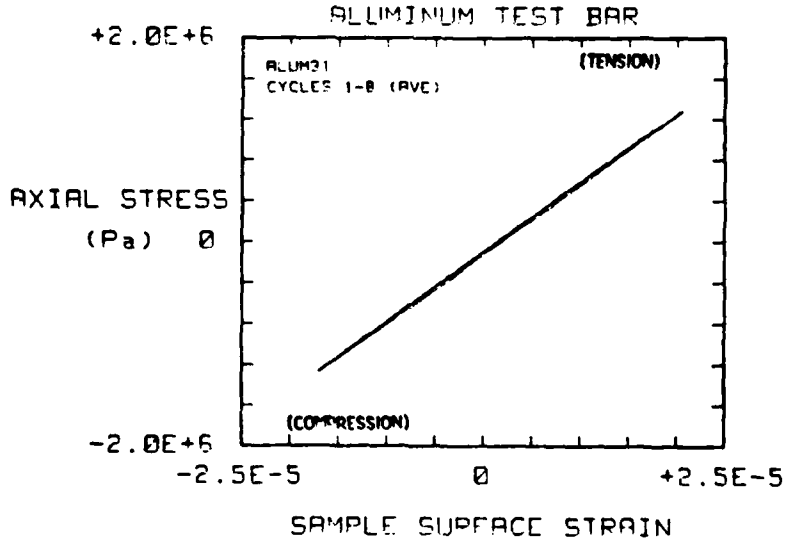

Fig. 4.1 Stress-strain response for aluminum test bar.

Experimental results also show that each rock displays nearly linear behavior when the loading is very small, around 4.5×10^4 Pa, resulting in strains between 2×10^{-6} and 6×10^{-6}, depending on rock type (Figs. 4.2 through 4.5). At higher load levels (Figs. 4.6-4.9) there is evidence of

strong nonlinearity and inelasticity in the weakest frame rock, Berea sandstone, while the nonlinear and inelastic effects are more subtle in the stronger frame rocks, especially Indiana limestone. In all rock specimens except Indiana limestone the effective modulus of the rock is significantly larger in compression than in tension. In two anomalous cases, Indiana limestone and Westerly granite have a slightly higher modulus in tension than in compression at rather small loads (Fig. 4.10).

McKavanagh and Stacey (1974) argue that it is possible to distinguish between linear anelastic relaxation and nonlinear relaxation, such as intergranular friction, by examining the shape of the hysteresis loop tips. Cusped tips indicate a nonlinear mechanism, while rounded tips indicate linear anelastic relaxation. Expanded views of the hysteresis loop tips measured on Westerly granite, Boise sandstone, and Berea sandstone are shown in Figs. 4.11, 4.12, and 4.13, respectively. In each case the tips are cusped and not rounded, which argues against an anelastic relaxation mechanism.

In some cases evidence for large nonrecoverable changes in the rock during the first excursion to a "new" maximum load is clear. A reasonable assumption is that these changes are associated with intergranular cracking. This is apparent when the hysteresis loop is not clearly established until at least the second cycle of loading. In the case of Berea sandstone subjected to 1.25×10^5 Pa axial stress (Fig. 4.14), the result of the first full loading cycle was a net shortening of the specimen. The nonrecoverable change at comparable stress is small in rocks with a moderately strong frame, such as Boise sandstone and Westerly granite (Figs 4.15 and 4.16). Indiana limestone, the rock with the strongest frame, shows no hysteresis and no nonrecoverable changes after comparable loading (Fig 4.17).

SC5361.8SA

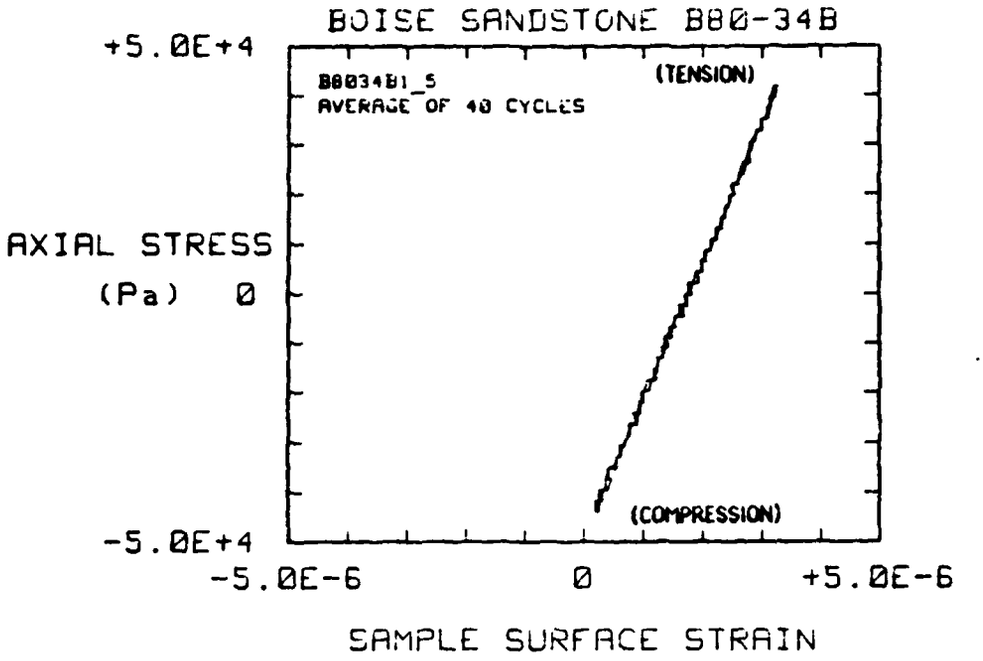

Fig. 4.2 Stress-strain response for Boise sandstone with a peak loading stress of 4.5×10^4 Pa showing nearly linear behavior.

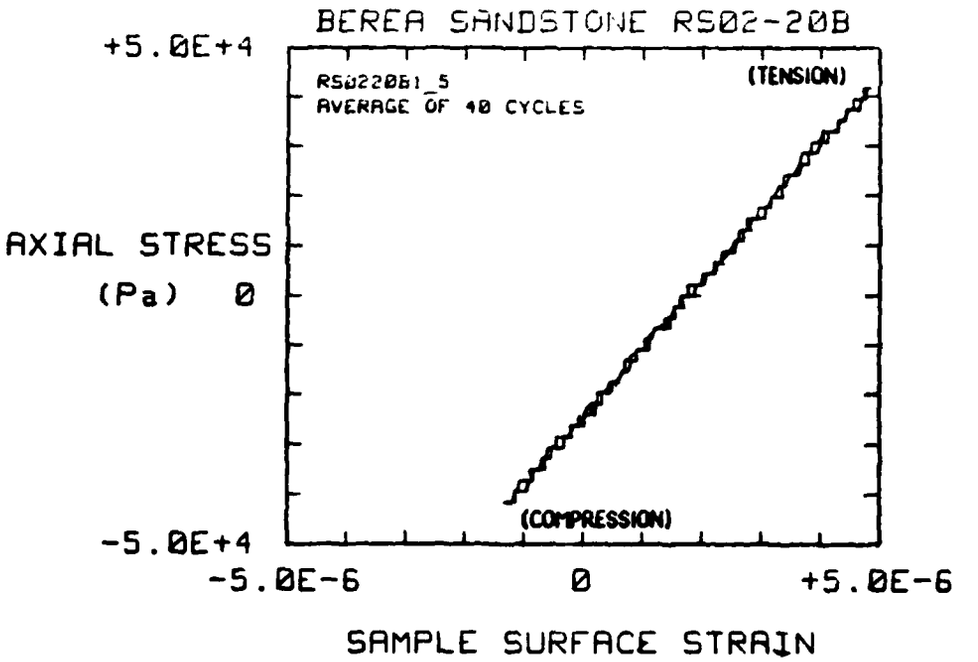

Fig. 4.3 Stress-strain response for Berea sandstone with a peak loading stress of 4.5×10^4 Pa showing nearly linear behavior.

SC5361.8SA

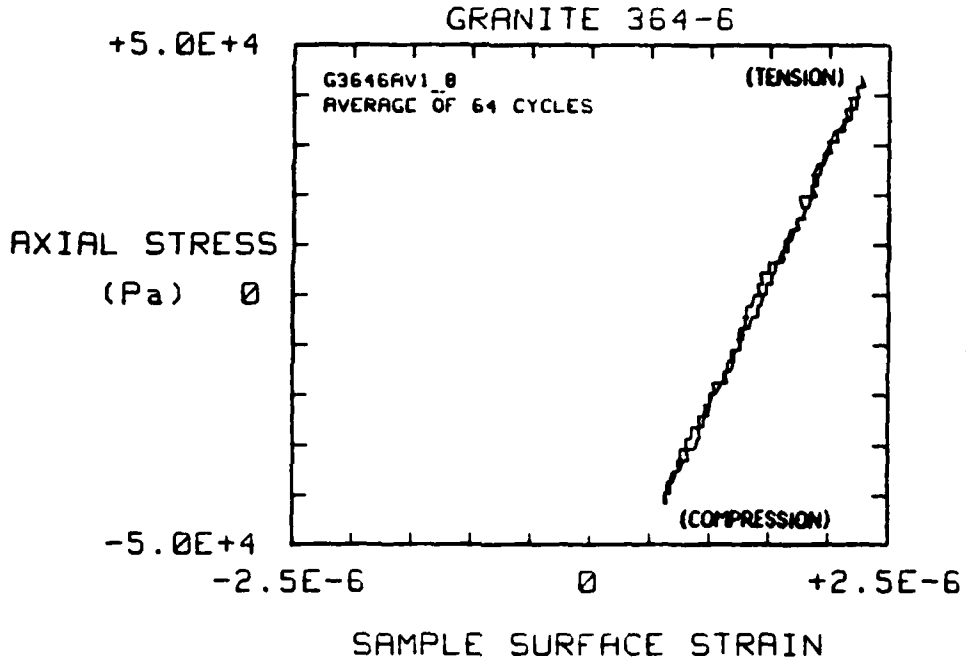

Fig. 4.4 Stress-strain response for Westerly granite with a peak loading stress 4.5 × 10^4 Pa showing nearly linear behavior.

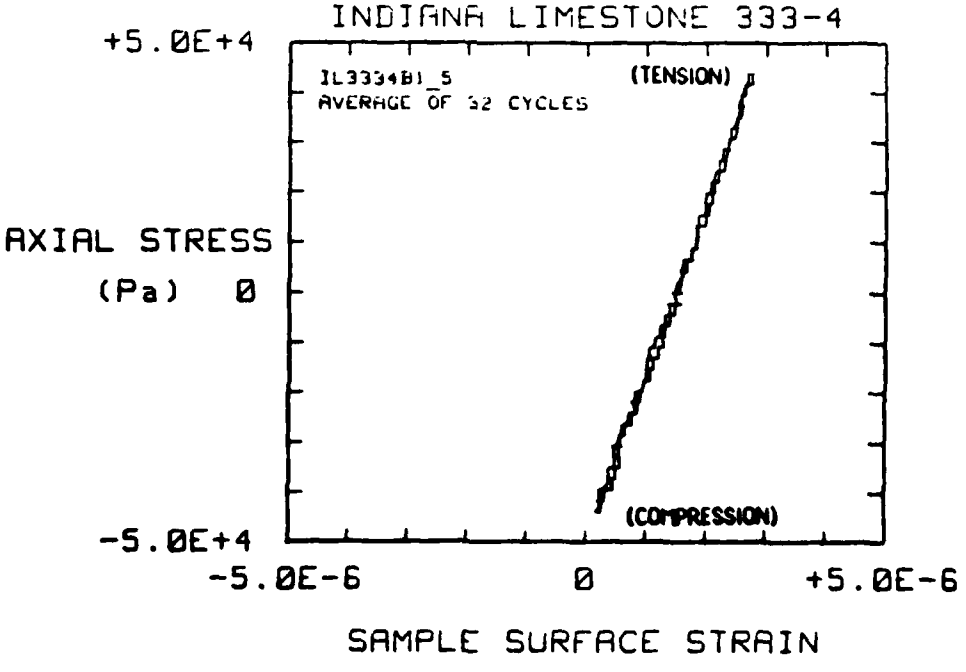

Fig. 4.5 Stress-strain response for Indiana limestone with a peak loading stress of 4.5 × 10^4 Pa showing nearly linear behavior.

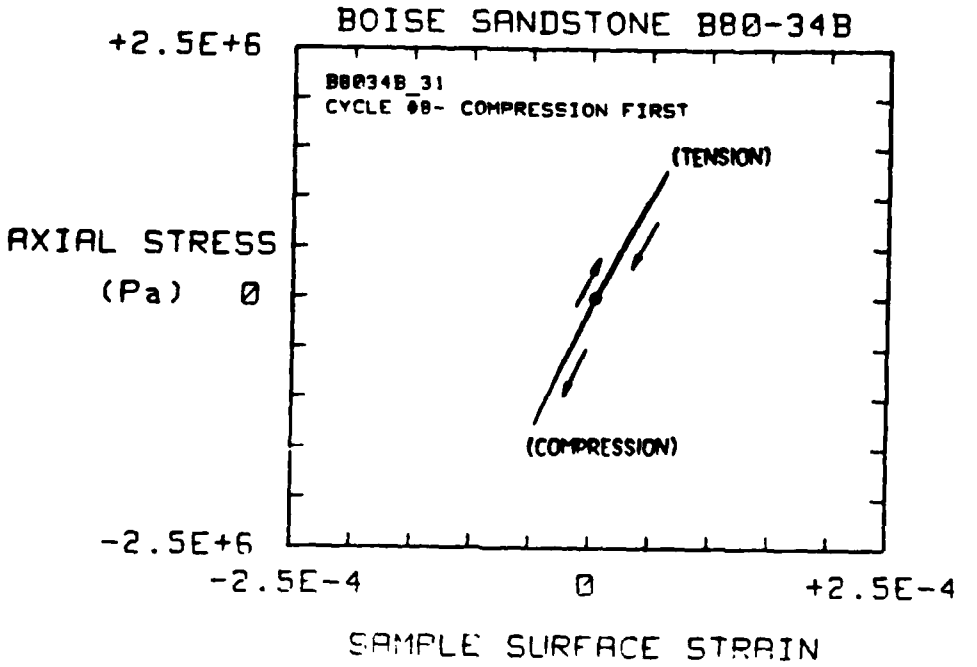

Fig. 4.6 Stress-strain response for Boise sandstone with a peak loading stress of 4.5×10^4 Pa.

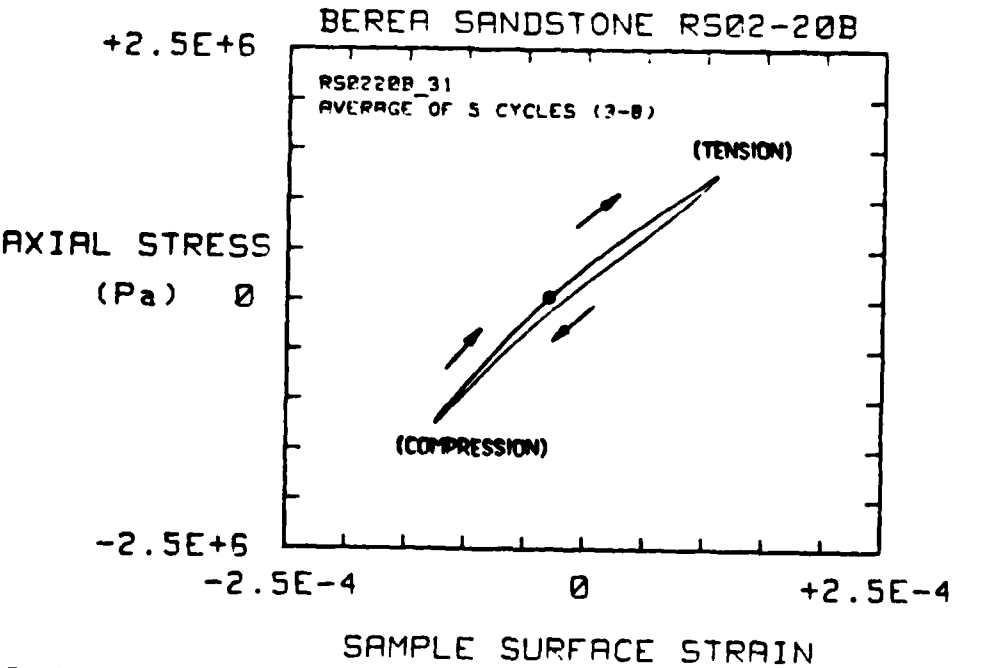

Fig. 4.7 Stress-strain response for Berea sandstone with a peak loading stress of 1.32×10^6 Pa.

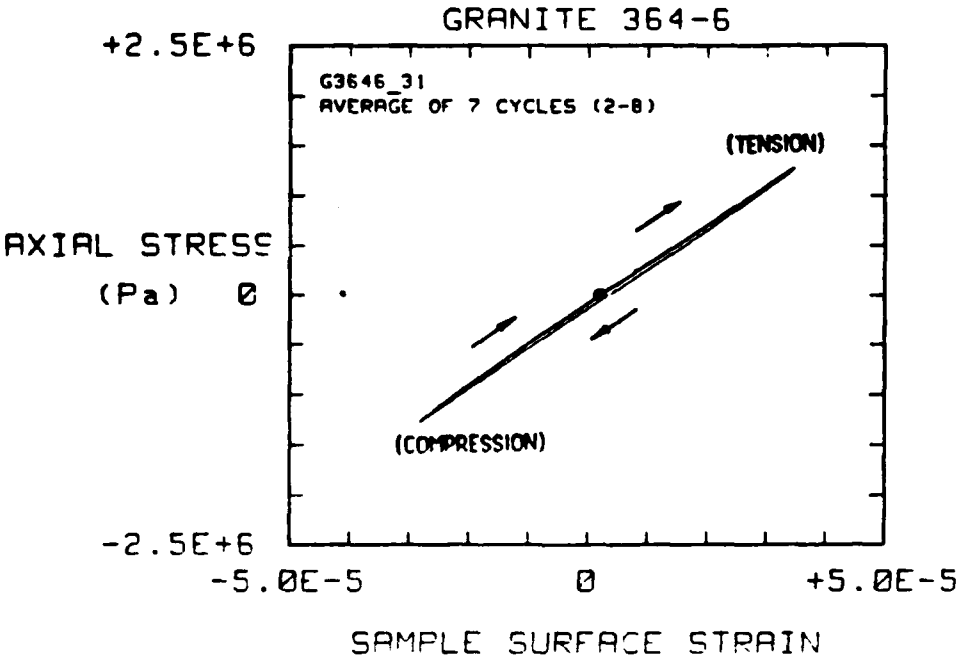

Fig. 4.8 Stress-strain response for Westerly granite with a peak loading stress of 1.32×10^6 Pa.

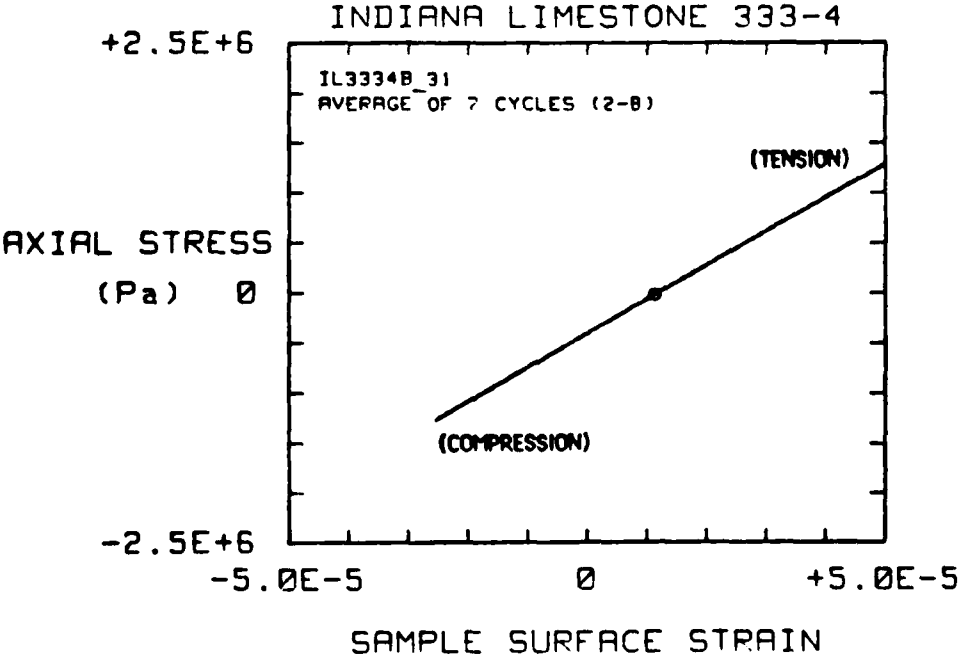

Fig. 4.9 Stress-strain response for Indiana limestone with a peak loading stress of 1.32×10^6 Pa.

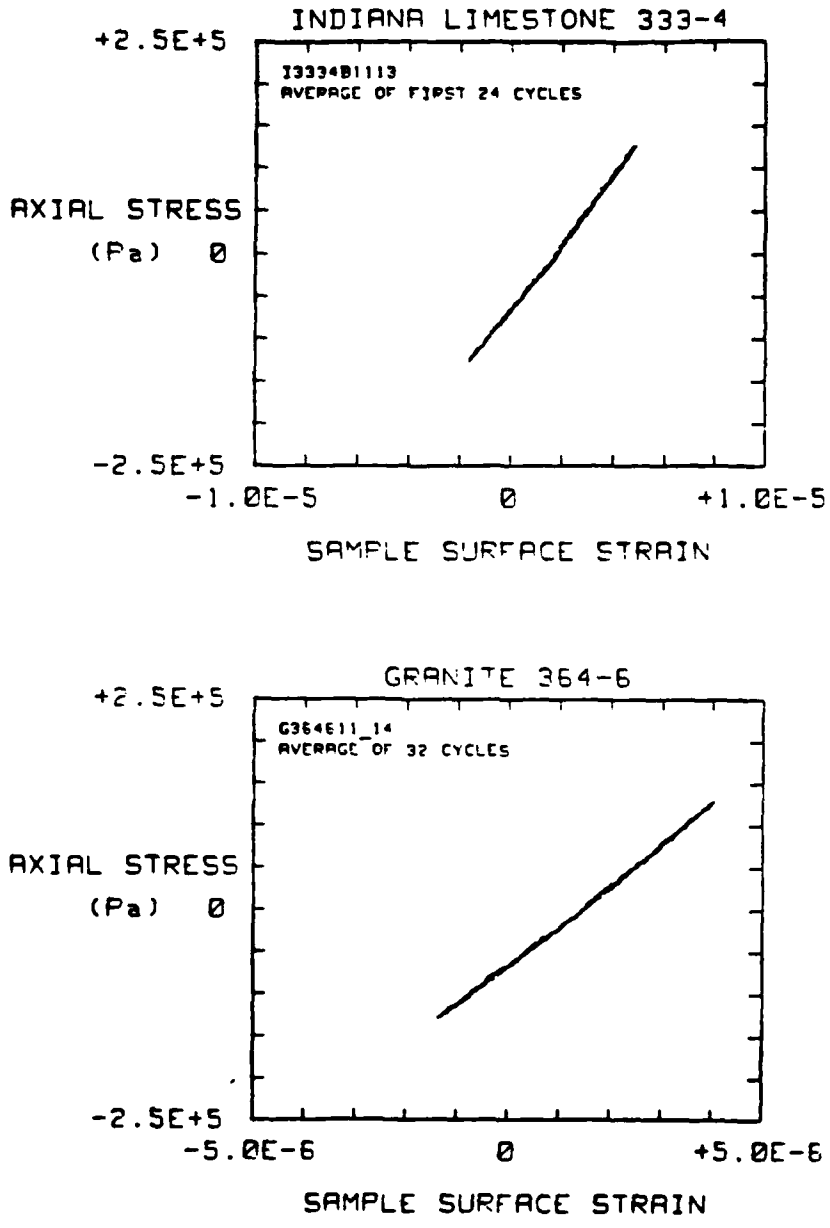

Fig. 4.10 Stress-strain response for two rocks showing the anomalous occurrence of a slightly higher effective modulus in tension than in compression. Peak loading stresses are relatively small (1.32×10^5 Pa).

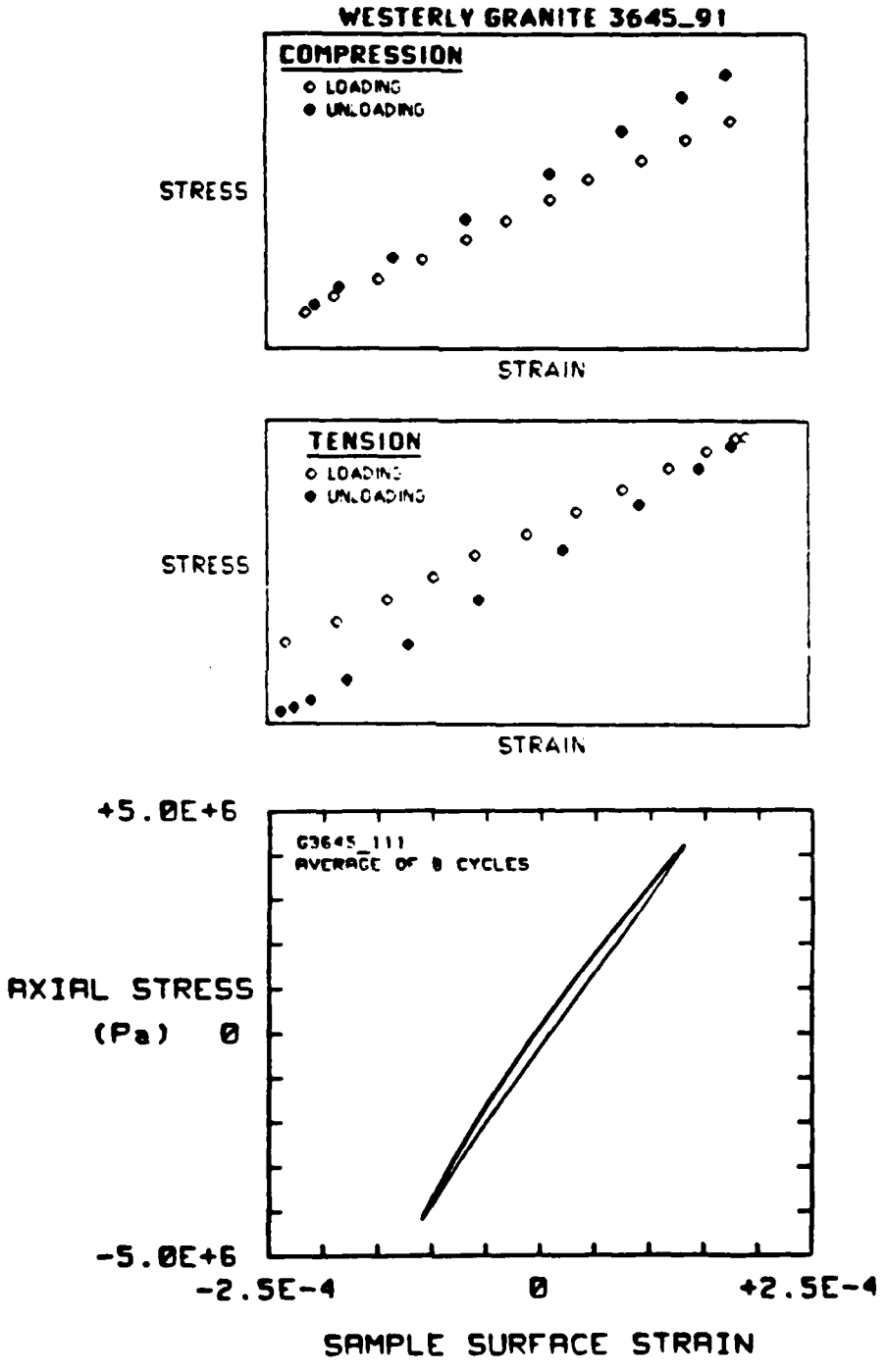

Fig. 4.11 Magnified views of the hysteresis loop tips for Westerly granite.

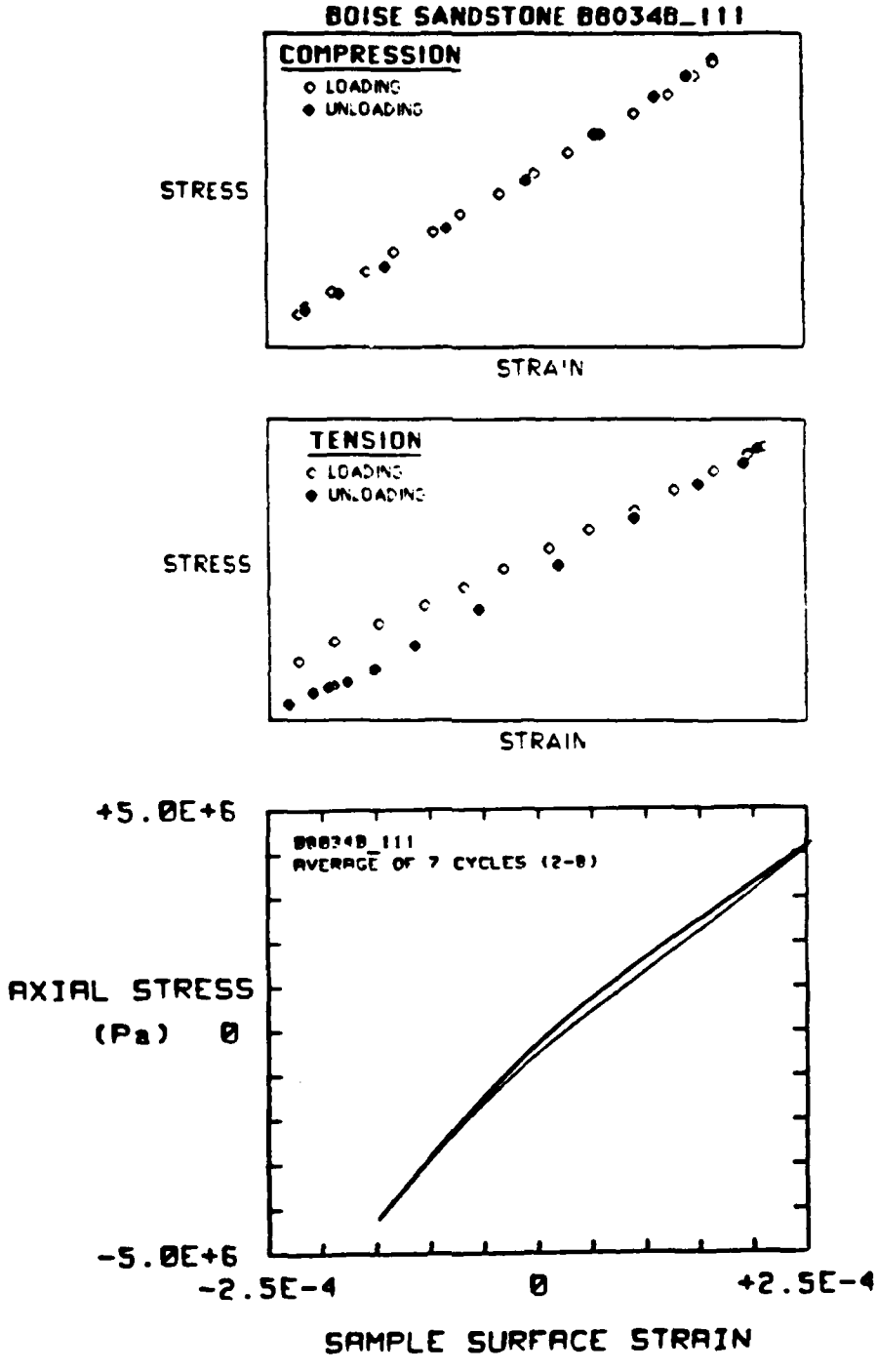

Fig. 4.12 Magnified views of the hysteresis loop tips for Boise sandstone.

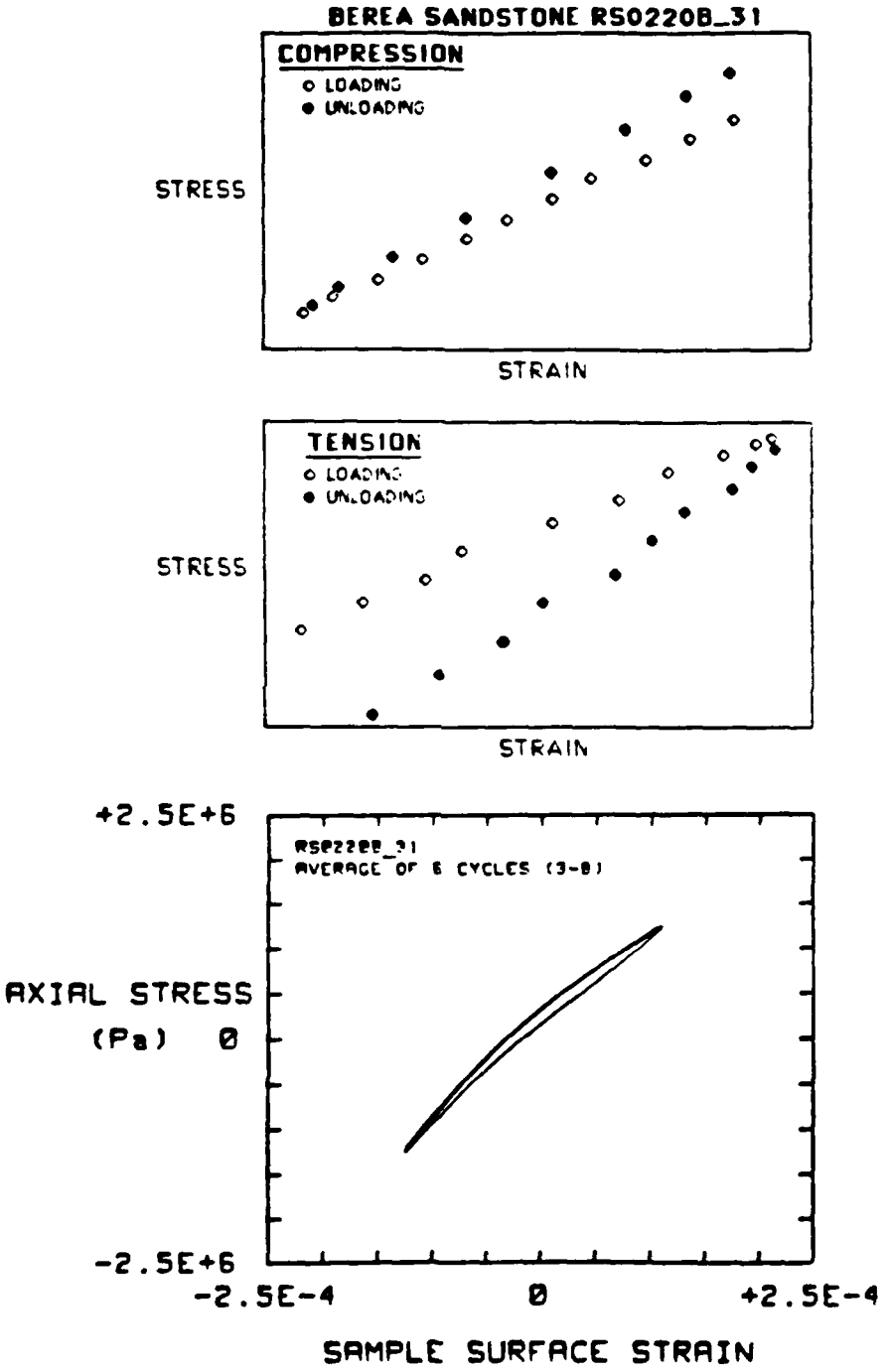

Fig. 4.13 Magnified views of the hysteresis loop tips for Berea sandstone.

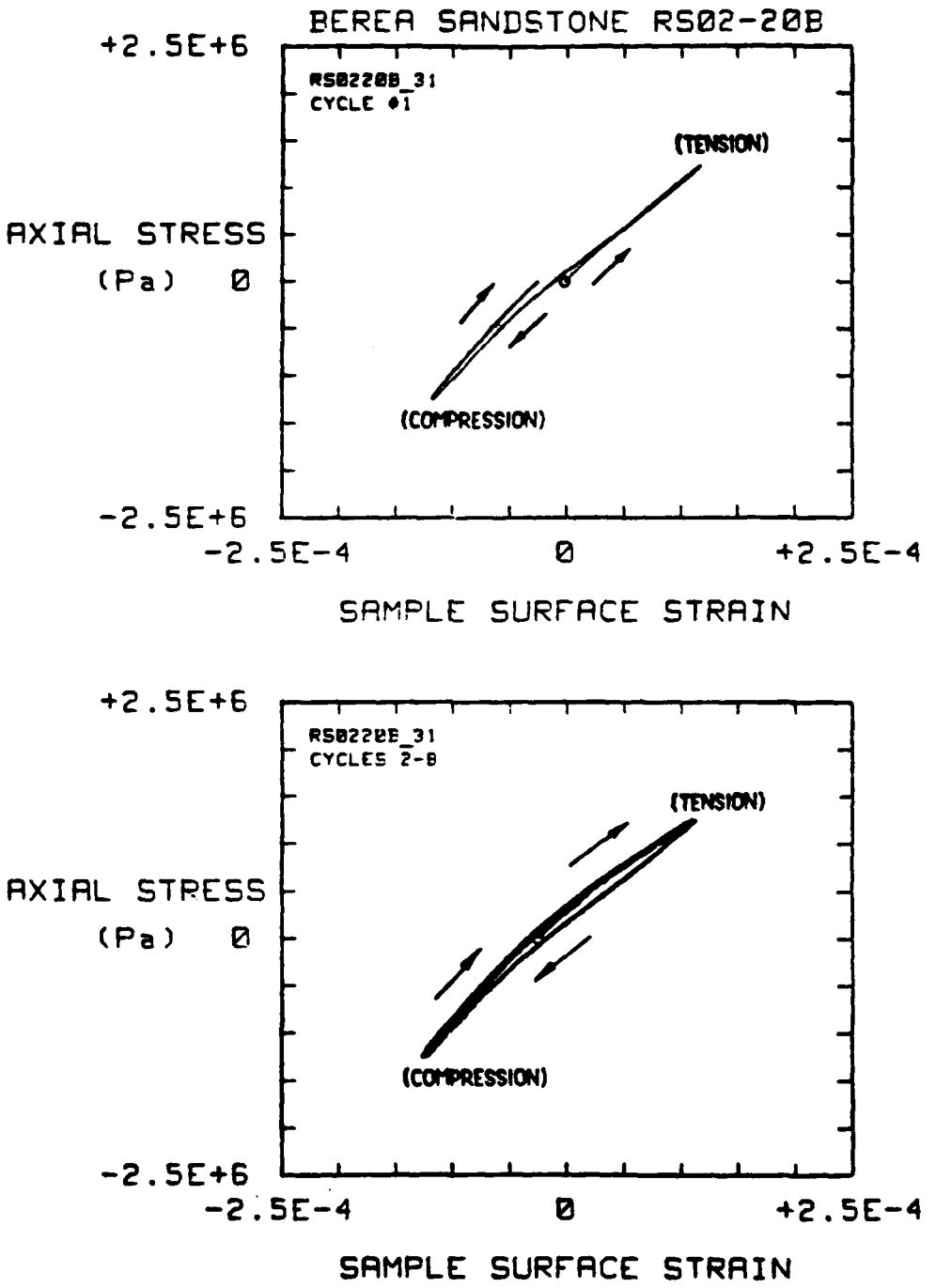

Fig. 4.14 Comparison of the first loading cycle for Berea sandstone at 1.25×10^6 Pa with the subsequent 7 cycles showing nonrecoverable changes after the first. The previous maximum load was 4.39×10^5 Pa.

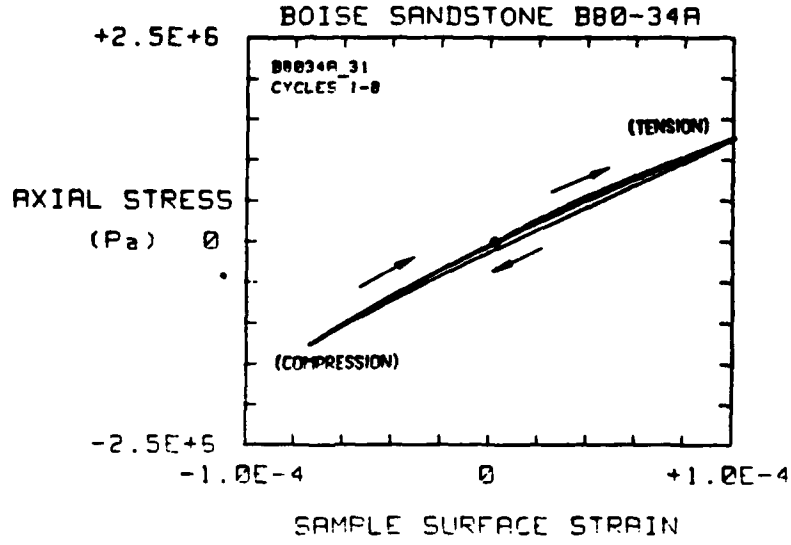

Fig. 4.15 Stress-strain response for the first eight loading cycles for Boise sandstone at 1.25×10^6 Pa. A small amount of nonrecoverable change is observed after the first cycle, but the following seven are superimposed. The previous maximum load was 4.39×10^5 Pa.

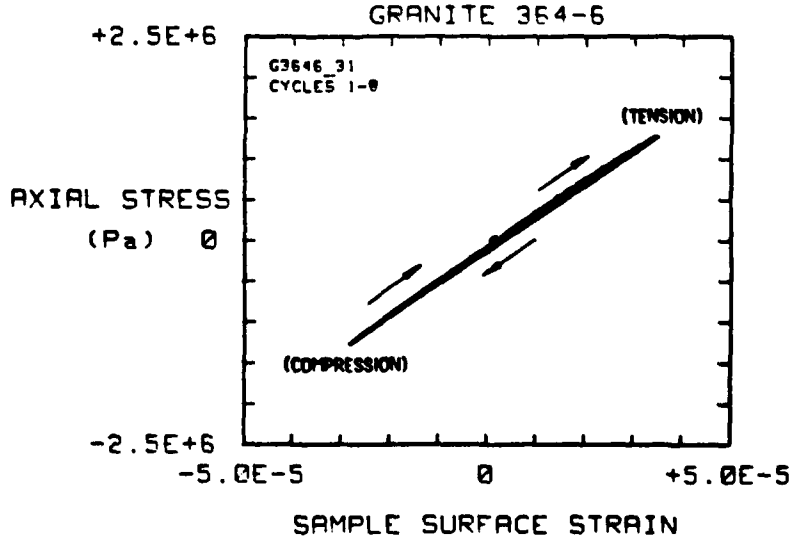

Fig. 4.16 Stress-strain response for the first eight loading cycles for Westerly granite at 1.25×10^6 Pa. A small amount of nonrecoverable change is observed after the first cycle, but the following seven are superimposed. The previous maximum load was 4.39×10^5 Pa.

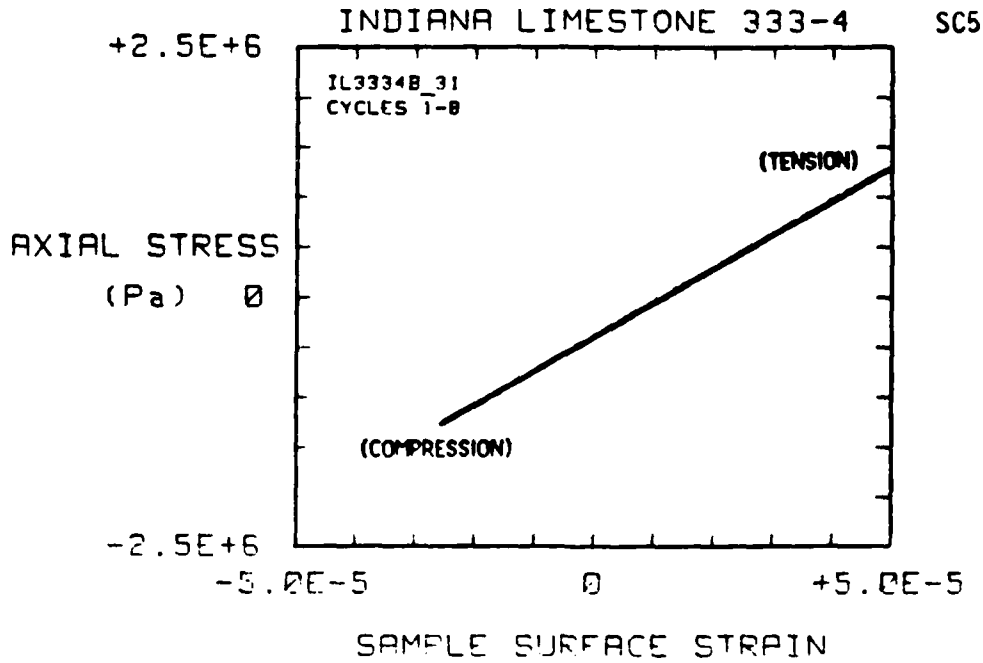

Fig. 4.17 Stress-strain response for the first eight loading cycles for Indiana limestone at 1.25×10^6 Pa. The material appears to be nearly linear elastic and nonrecoverable changes are not observed.

By reversing the direction of initial loading, the shape of tensional hysteresis loops and compressive hysteresis loops can be examined. In Figs. 4.18 and 4.21 we show the effects of reversing the loading direction from tension-first to compression-first, and from compression-first to tension-first, respectively, for two different rock types. It is apparent that in Boise sandstone the opening of the loop is due primarily to tensile stresses, and that the behavior in compression is nearly nonlinear elastic. In Westerly granite these effects are similar, but the contrast between compressional hysteresis and tensional hysteresis is less pronounced. A hysteresis loop exists in both compression and tension, but it is smaller in compression.

Finally, the effect of frequency on the shape of the hysteresis loop has been examined. The results of measurements on Boise sandstone and Westerly granite at 1 Hz and at 0.1 Hz are shown in Figs. 4.22 and 4.23. The curves superimpose very well, which is consistent with a frictional relaxation mechanism, even though this observation alone does not preclude anelastic relaxation.

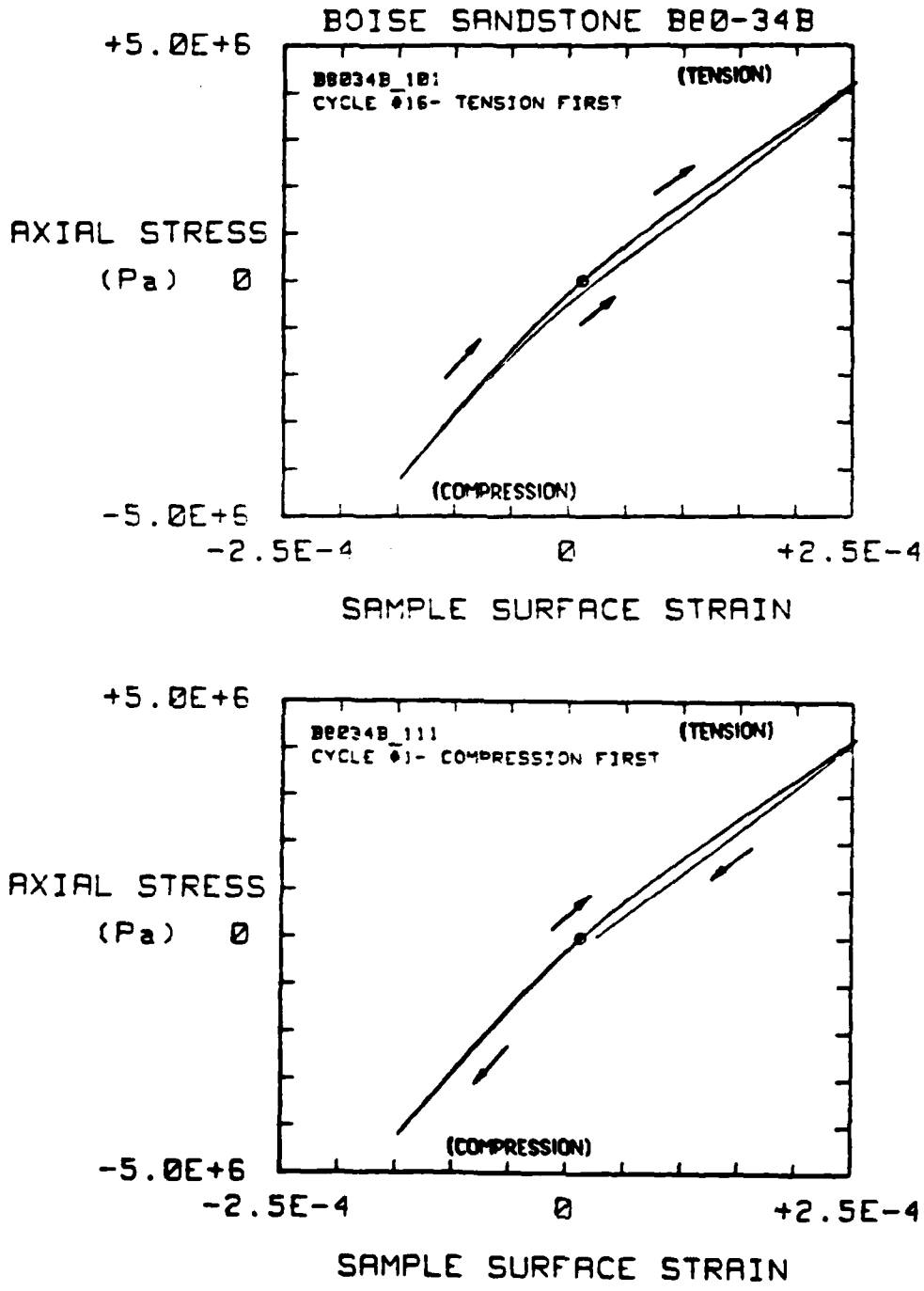

Fig. 4.18 Effect of reversing the initial loading direction from tension-first to compression-first for Boise sandstone with a maximum loading stress of 4.39×10^6 Pa, showing the lack of significant hysteresis in the compressional part of the cycle.

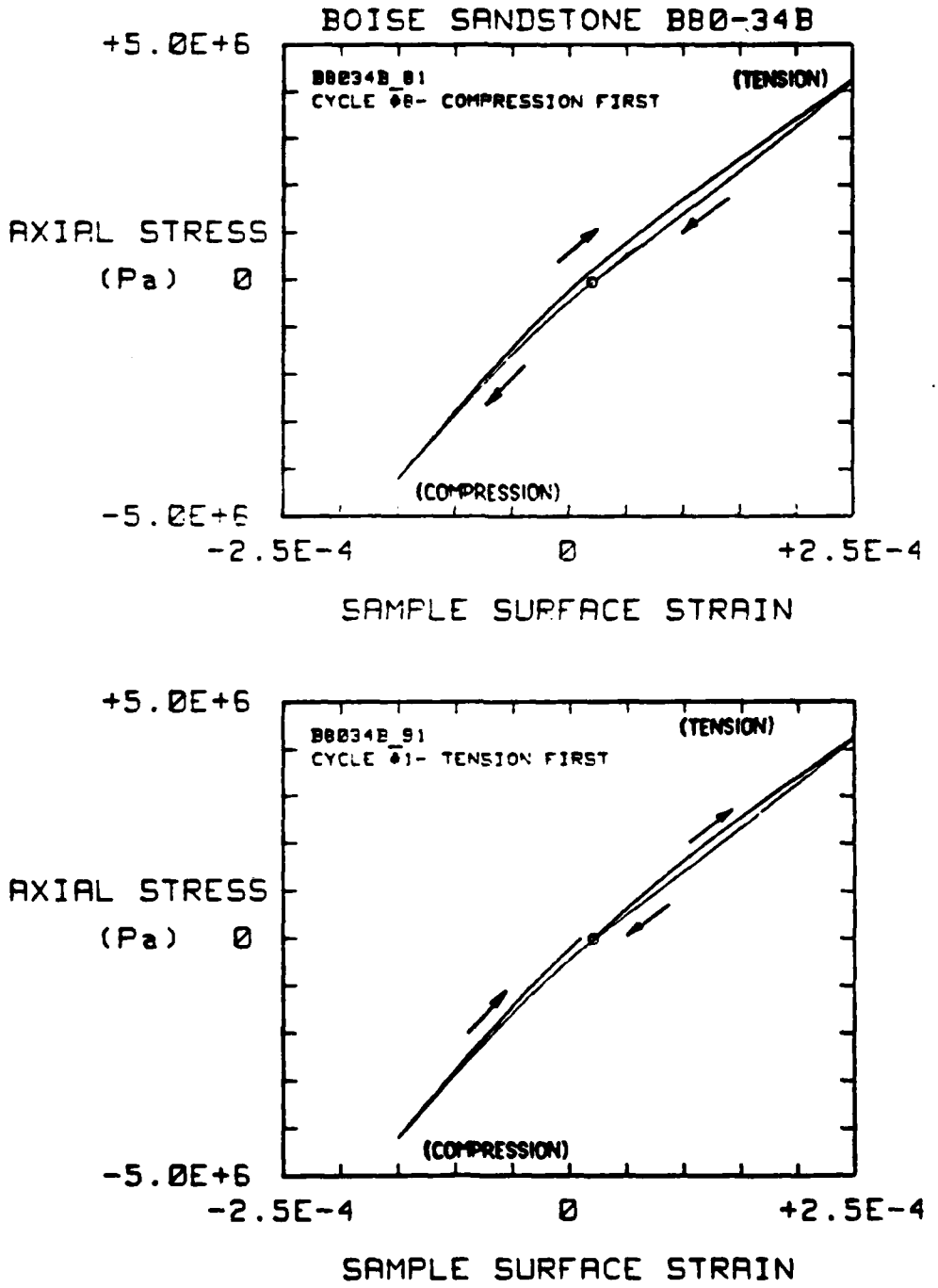

Fig. 4.19 Effect of reversing the initial loading direction from compression-first to tension first for Boise sandstone with a maximum loading stress of 4.39×10^6 Pa, showing the development of a hysteresis loop in tension.

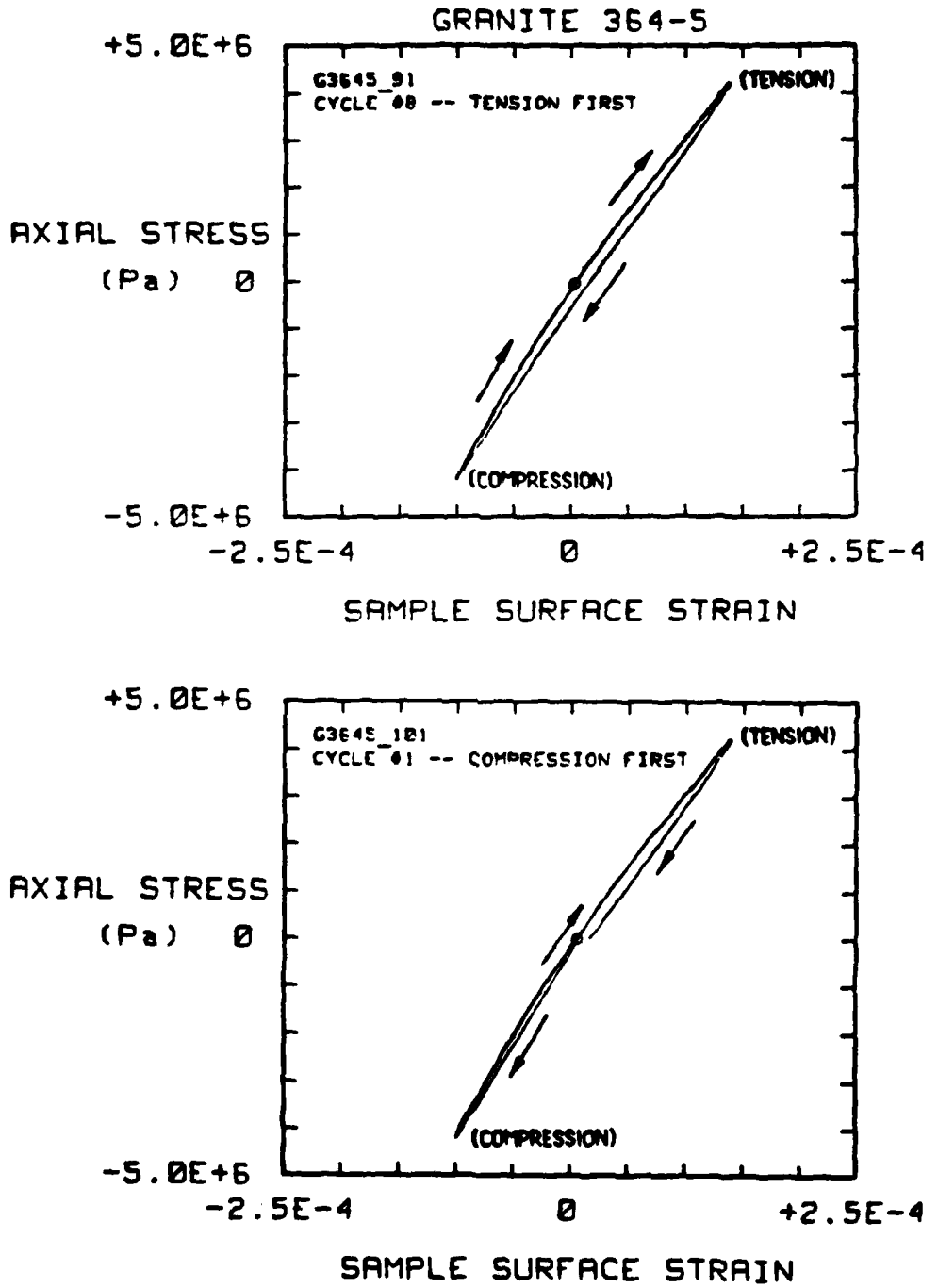

Fig. 4.20 Effect of reversing the initial loading direction from tension-first to compression-first for Westerly granite with a maximum loading stress of 4.39×10^6 Pa, showing a significant compressional hysteresis loop.

SC5361.8SA

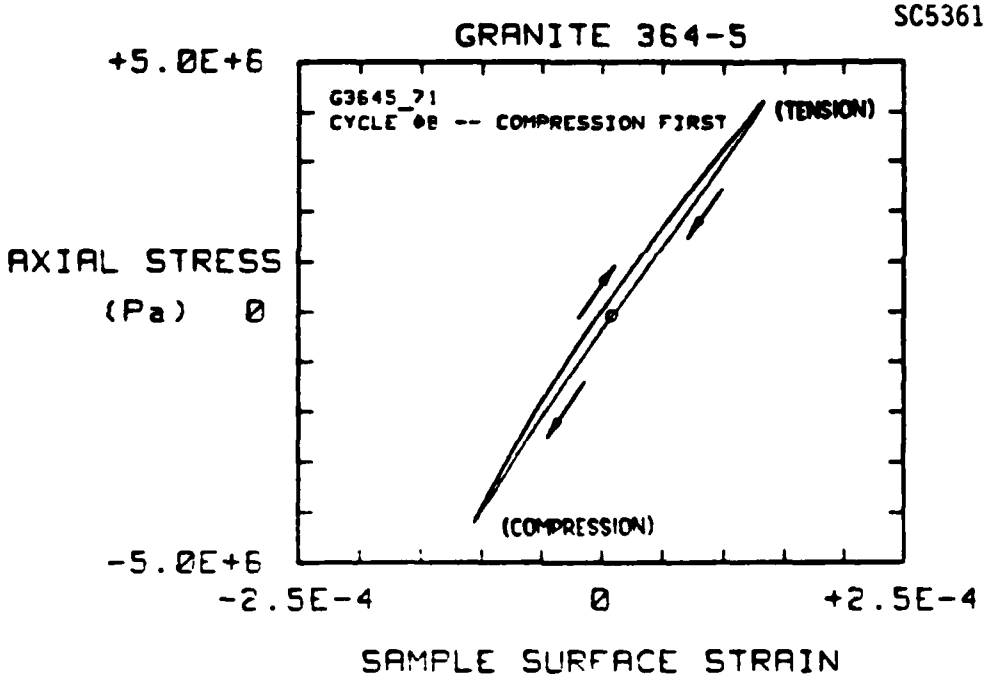

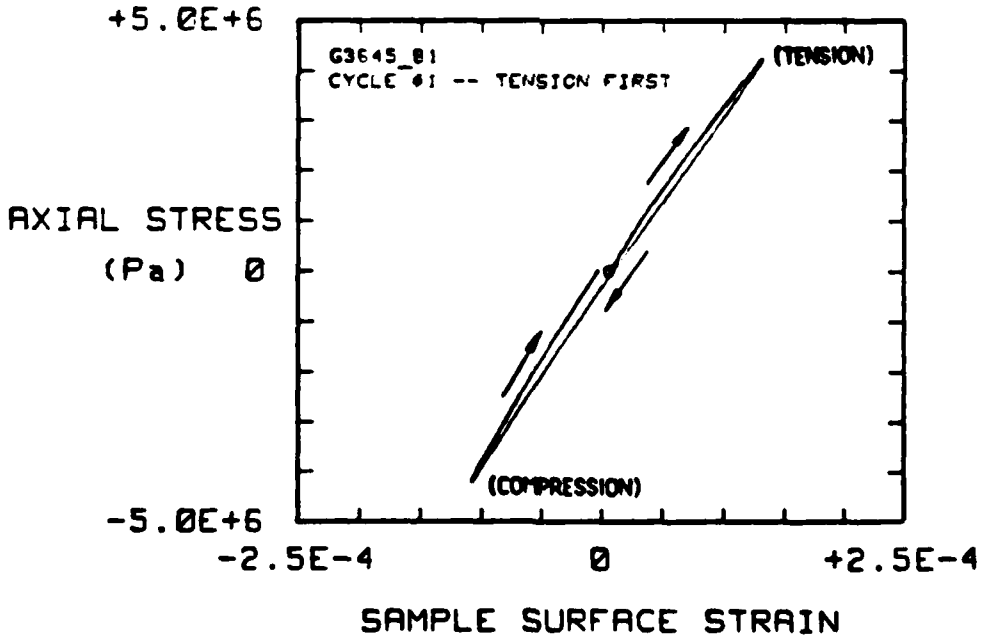

Fig. 4.21 Effect of reversing the initial loading direction from compression-first to tension-first for Westerly granite with a maximum loading stress of 4.39×10^6 Pa. Figure shows the existence of a hysteresis loop in tension which is larger than the compressional hysteresis loop illustrated in Fig. 4.20.

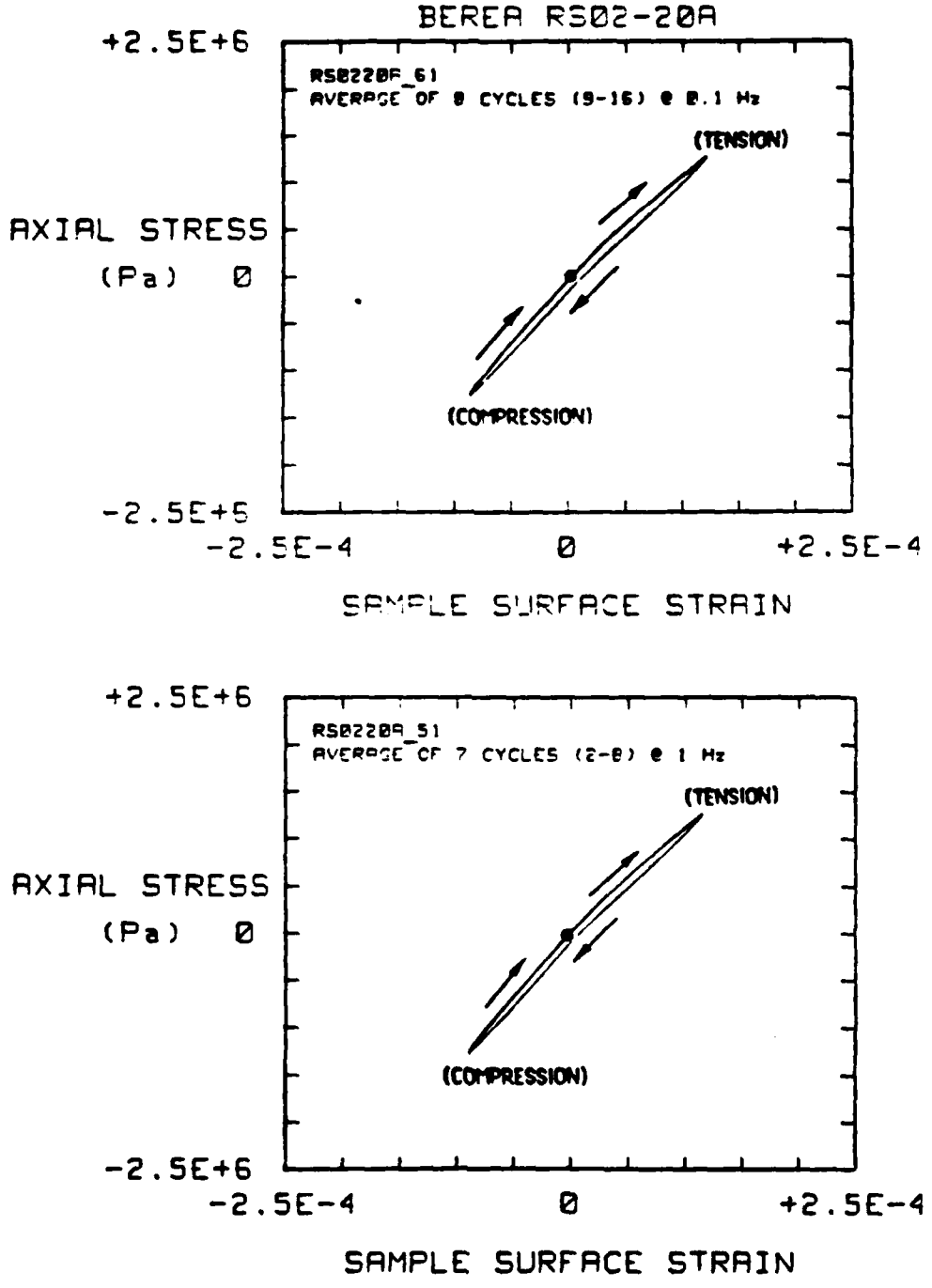

Fig. 4.22 Comparison of the stress-strain response for Berea sandstone at two different frequencies. The traces appear to be identical.

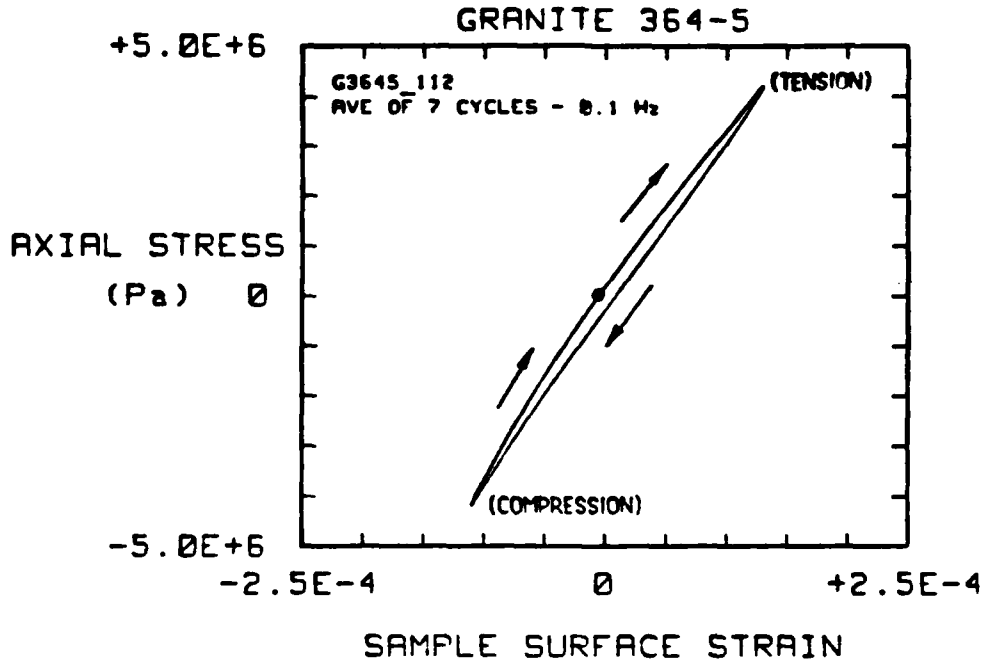

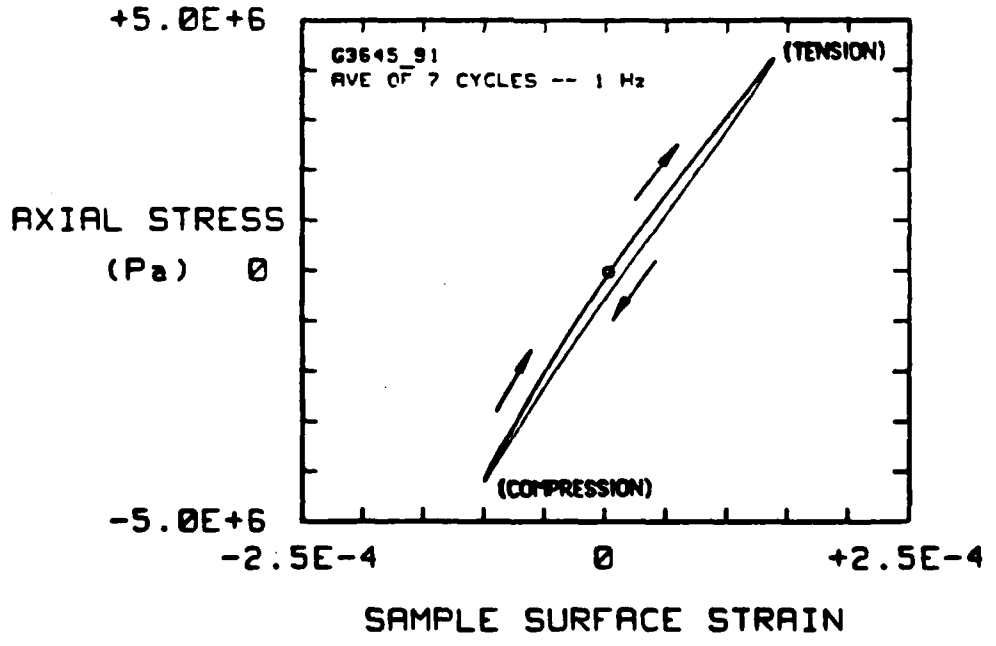

Fig. 4.23 Comparison of the stress-strain response for Westerly granite at two difference frequencies. The traces appear to be identical.

5.0 DISCUSSION AND CONCLUSIONS

In this study we have examined the details of stress-strain hysteresis loops when rock specimens are subjected to alternating compressive and tensile stresses. In general at nonlinear amplitudes the stiffness of the rock is greater in compression than in tension. Furthermore, preliminary results indicate that most of the energy loss during a full cycle of loading occurs as a result of strain in extension; the hysteresis loop in compression is smaller than the hysteresis loop in tension. The shape of the hysteresis loops also appears to be independent of frequency. These observations indicate a loss mechanism associated with intergranular friction. Intergranular sliding appears to be restricted by the impingement of opposing crack faces in compression, since the rock is stiffer in compression than in tension, and a large hysteresis loop develops only when the rock is subjected to tensile stresses.

The results of this study indicate that the mechanical behavior of rocks can be significantly different in compression than in tension and that the onset of nonlinear effects with increasing strain may not be the same for tensile loads as for compressive loads. All available evidence indicates that the primary relaxation mechanism at nonlinear amplitudes between 10^{-6} strain and 10^{-4} strain involves intergranular friction. More experimental work in this area will shed light on the issue of linearity vs nonlinearity at intermediate strains, and also will provide realistic detailed information about rock rheology for the numerical modeling of near-field seismic pulse propagation. For this work to be most meaningful true uniaxial strain is necessary, and specimens must be exposed to elevated confining pressures.

6.0 REFERENCES

1. Bache, T.C., W.J. Best, R.R. Blanford, G.V. Bolin, D.G. Harkrider, E.J. Herrin, A. Ryall and M.J. Shore (1981) A Technical Assessment of Seismic Yield Estimation, DARPA Report, January 1981.

2. Burdick, L.J., T. Wallace and T. Lay (1984a) Modeling Near-field and Teleseismic Observations from the Amchitka Test Site, Jour. Geophys. Res., 89, 4373-4388.

3. Burdick, L.J., T. Lay, D.V. Helmberger and D.G. Harkrider (1984b) Implication of Records from the Spall Zone of the Amchitka Tests to Nonlinear Losses in the Source Region and to Elastic Radiation by Spall. Annual technical report for the period November 15, 1982 to November 15, 1983. Prepared for the Advanced Research Projects Agency.

4. Gordon, R.B. and L.A. Davis (1968) Velocity and Attenuation of Seismic Waves in Imperfectly Elastic Rock, Jour. Geophys. Res., 73, 3917-3935.

5. Mavko, G.M. (1979) Frictional Attenuation: An Inherent Amplitude Dependence, Jour. Geophys. Res., 84, 4769-4775.

6. McCarter, G.D. and W.R. Wortman (1985) Experimental and Analytic Characterization of Nonlinear Seismic Attenuation, Final Report for the Period March 21, 1984 through March 20, 1985. Prepared for the Advanced Research Projects Agency.

7. McKavanagh, B. and F.D. Stacey (1974) Mechanical Hysteresis in Rocks at Low Strain Amplitudes and Seismic Frequencies, Phys. Earth Planet. Interiors, 8, 246-250.

8. Minster, J.B. and S.M. Day (1985) Decay of Wavefields Near an Explosive Source Due to High-Strain, Nonlinear Attenuation, Unpublished Manuscript.

9. Perret, W.R.(1967) Free-Field Particle Motion from a Nuclear Explosion in Salt, Part I, Project Dribble, Salmon Event, VUF-3012, Sandia Laboratory.

10. Shock, R.N. and H. Louis (1982), Strain Behavior of a Granite and a Graywacke Sandstone in Tension, Jour. Graphys. Res., 87, 7817-7823.

11. Stewart, R.R., M.N. Toksoz, and A. Timur (1983) Strain Dependent Attenuation: Observations and a Proposed Mechanism, Jour. Geophys. Res., 88, 546-554.

12. Tittmann, B.R. (1983) Studies of Absorption in Salt, Final Report for the period December 1, 1981 through November 30, 1982, Prepared for Air Force Office of Scientific Research.

13. Tittmann, B.R. (1984a) Non-linear Wave Propagation Study, Semi-annual technical report no. 1 for the period June 1, 1983 through November 30, 1983, Prepared for Air Force Office of Scientific Research.

14. Tittmann, B.R. (1984b) Non-linear Wave Propagation Study, Semi-annual technical report no. 2 for the period December 1, 1983 through May 31, 1984, Prepared for Air Force Office of Scientific Research.

15. Trulio, J.G. (1978) Simple Scaling and Nuclear Monitoring, Final Report of DARPA supported research program, April 1978.

16. Trulio, J.G. (1981) State-of-the-Art Assessment: Seismic Yield Determination, in A Technical Assessment of Seismic Yield Estimation, DARPA Report Appendix, January 1981.